

Pulsed Nd:YAG Laser Micro-turning Process of Alumina Ceramics

G. Kibria, B. Doloi and B. Bhattacharyya

Abstract Laser micro-turning process is one of the new and emerging technologies in the area of laser material processing (LMP) of engineering materials. It is employed for generation of micro-turning surface of particular surface profile and dimensional accuracy on cylindrical workpiece with specific length and depth of turn within tight tolerance. As the process is recently developed micro manufacturing technique, a well planned research study and experimental investigation should be conducted considering various laser micro-turning process parameters. Therefore, various experimental schemes are adapted to study and analysis of significant process parameters on response criteria such as surface roughness and machining depth. A servo controller based fixture is designed and developed indigenously to hold and rotate the cylindrical shaped work samples at various *workpiece rotating speed*. Overlap between two successive spots (i.e. *spot overlap*) and overlap between two successive micro-groove widths (i.e. *circumferential overlap*) play major role for generating quality surface features during laser micro-turning process. Therefore, mathematical formulations of *spot overlap* and *circumferential overlap* are developed for better understanding of the laser micro-turning process and also to study the effects of these overlap factors on performance characteristics. Moreover, attempt has been made to carry out experimental investigation to micro-turn cylindrical shaped engineering ceramics at laser defocus conditions of laser beam. Moreover, comparative study and analyse is performed to explore the effect of focused and defocused conditions of laser beam on surface roughness criteria. SEM micrographs of the laser turned surface captured at various parametric combinations have also been studied for qualitative analysis of the process.

G. Kibria (✉)

Department of Mechanical Engineering, Aliah University, Kolkata 700156, India
e-mail: prince_me16@rediffmail.com

B. Doloi · B. Bhattacharyya

Department of Production Engineering, Jadavpur University, Kolkata 700032, India
e-mail: bdoloionline@rediffmail.com

B. Bhattacharyya

e-mail: bb13@rediffmail.com

© Springer India 2015

S.N. Joshi and U.S. Dixit (eds.), *Lasers Based Manufacturing*,
Topics in Mining, Metallurgy and Materials Engineering,
DOI 10.1007/978-81-322-2352-8_18

343

Keywords Laser micro-turning process • Alumina (Al_2O_3) • Surface roughness • Defocusing conditions • Pulsed Nd:YAG laser • Spot overlap • Circumferential overlap

1 Introduction

Increased interest in micromachining technology has captured the imagination of every manufacturing and industry segment such as aerospace, medical appliance and automotive as well as military applications. The potential for product miniaturization continues to grow and while posing numerous technical challenges. In response to this continued miniaturization, researchers are developing new technologies to meet the high demands of miniature products and unique challenges posed by micro manufacturing and must develop appropriate micromachining systems or processes to support this growth. Several micro-machining technologies are being employed in the manufacture of a wide variety of micro-products and devices. Manufacturing techniques, both traditional and non-traditional, have been developed significantly for the realization of diverse range of microstructures used for various micro-system applications. Demand for various micro-features in macro as well as micro-components has necessitated the urgent need to develop and employ a number of alternative manufacturing techniques, other than traditional processes, so that a wide range of materials such as ceramics, polymer, composites, high strength temperature resistant (HSTR) alloys can be used as parent material for micro-components or parts. Non-traditional micro-machining processes can be efficiently and effectively applied to machine these types of hard-to-machine materials irrespective of their hardness, toughness and brittleness. Laser beam machining (LBM) is one of the advanced non-traditional machining processes, which can be applied to manufacture wide variety of geometries and complex shapes on difficult-to-machine materials with greater accuracy and faster rate.

Laser beam machining is classified based on type of source, mode of operations and wavelength. Among a wide variety of lasers, Nd:YAG lasers, Excimer lasers and Diode lasers are widely used for micro-machining applications. In pulsed mode, the vaporization of material occurs in a very short time duration so that it does not allow the heat to be conducted into the bulk material. The pulsing of laser beam is done in various ways, such as normal pulsing, Q-switching and mode locking. Nd:YAG laser compiled with Q-switch pulsing offers outstanding features and quality of machining during laser micro-machining operations such as micro-cutting, micro-drilling, micro-grooving, micro-turning and micro-milling.

Among the various micro-machining techniques of laser beam machining processes, laser micro-turning process is a newly developed machining process in the modern cutting-edge technology era. In this innovative technique of micro-machining process, cylindrical surface of engineering ceramics and composites can be micro-turned with high accuracy and good quality surface. Moreover, laser

micro-turning process using pulsed Nd:YAG laser has machining features including melting and vaporization of material in very short time that avoids formation of recast/re-solidified layer on machined surface and high repetition rate machining that avoids cracks in machined surfaces and sub-surfaces. By taking into account all these significant advantages, this new micro-machining technique i.e. laser micro-turning process can be employed to remove very thin layer (depth) from cylindrical work-piece of ceramics, which are difficult-to-turn in conventional turning processes. By this process, one can produce desired dimensional micro-grooves or slots for a specific depth and length on cylindrical surface. This kind of micro-turned surface with specific surface texture is required for assembly purpose of various micro-parts in the micro-engineering applications. In ceramic whistle stud assembly purpose, high-alumina ceramic spikes are often used. In lining applications, the alumina ceramic bearing rings are also being used for assembling several precision components. Further, on the shop floor, the reduction of the number of micro cutting edges of ceramic grinding wheel due to worn out of abrasive particles from the wheel surface is a major problem. The generation of micro-cutting edges on grinding wheel is a major challenge for the manufacturing technocrats of high precision industries. Laser micro-turning process can be a novel technology to generate new cutting edges of desired surface topography on grinding wheel surface.

2 Laser Micro-turning Process

In 1988, three dimensional laser beam machining technology was introduced for removal of material in bulk mode while using two intersecting laser beams (Chrysolouris et al. 1988). However, to produce a laser turned surface of a specific length and micron sized depth or to machine micro-groove for a specific length, the use of two intersecting beam fails. Most of the past research works are related to laser micro-drilling and micro-grooving operations of structural ceramics such as Si_3N_4 , Al_2O_3 , MgO and SiC (Dahotre and Harimkar 2008; Kibria et al. 2010a). In the area of laser micro-turning process, few research investigation has been reported in the literature. On the other hand, Aluminium Oxide (Al_2O_3) ceramic is one of the most important technical ceramics, which are being utilized in several applications ranging from automotive (bearing, valve, etc.), biomedical (orthopedic implants particularly in hip replacement surgery) to aerospace (seals for gas turbine engines, fuel line assembly, and thermocouples) and military (modern weapons, ceramic armor, etc.) due to its several properties like high mechanical strength, the ability to retain dimensional stability and excellent chemical resistance in aggressive environments (Basu and Balani 2010; Gitzen 1970; Kim et al. 2009). In many applications, micro-turning process is carried out using diamond tool for processing hard-to-machine cylindrical shaped materials. Yet, the use of diamond tool calls upon many limitations while machining of advanced ceramics and composites. Firstly, the diamond tool may undergo irregular and excessive wear as it is a contact-type machining process and it further results in uneconomic production and

also cracks formation on the machined surface and sub-surface due to brittle nature of ceramic materials (Buttery et al. 1979; Shih 2000). In addition, wire electrical discharge turning (WEDT) process is a very recently developed novel micro-turning technology used for fabricating micro-structures like small-pins, micro-tool electrodes etc. (Haddad et al. 2008, 2010). However, in this process, non-conductive materials like ceramics cannot be used as workpiece materials. Laser micro-turning process, which removes materials layer-by-layer from cylindrical shaped work sample, can be effectively utilized to generate such micro-turning surface or micro-groove on difficult-to-machine materials. The basic concept of laser micro-turning process is of producing multiple side-by-side micro-grooves, where each groove width makes certain amount of overlap with previous one (Kruth et al. 2007). The amount of groove width overlap is controlled by two important process parameters of laser micro-turning process, namely axial feed motion (*Y feed rate*) and rotational speed of workpiece. To achieve a certain micro-turned depth and desired surface texture on the laser scanned surface, continuous scanning process of laser beam is carried out by focusing the beam on the preceding micro-turning surface. The amount of overlap between groove widths is measured in terms of *circumferential overlapping percentage* (CO_p), while the overlap between two consecutive spots is measured in terms of *spot overlapping percentage* (SO_p). The values of these two parameters are chosen so carefully that the percentage values lay more than 50 % to achieve quality surface during laser micro-turning operation. The laser spot diameter, *spot overlap*, *pulse frequency* and *linear scanning speed* are related as follow (Thawari et al. 2005)

$$(\text{Spot diameter}) \times (1 - \text{spot overlap}) \times (\text{pulse frequency}) = \text{linear speed} \quad (1)$$

Or,

$$\text{Spot overlapping percentage } (SO_p) = \left(1 - \frac{v}{D \times F_p}\right) \times 100\% \quad (2)$$

Here, v , D and F_p are *linear scanning speed* (mm/s), laser spot diameter (mm) and *pulse frequency* (Hz), respectively. By converting the *linear scanning speed*, v (mm/s) with *workpiece rotating speed*, N (rpm) and taking the diameter of workpiece as 10 mm, Eq. 2 can be written as

$$\text{Spot overlapping percentage } (SO_p) = \left(1 - \frac{0.5238 \times N}{D \times F_p}\right) \quad (3)$$

During laser beam scanning over the work surface, as shown in schematic view in Fig. 1, two successive spots 1 and 2 produce an overlap length of x . Due to Gaussian energy distribution of laser beam, the respective spots generate a small crater through melting and/or evaporation from irradiated spots. The micro-turned profile produced can be controlled by increasing the spot overlap area, i.e., increasing the *pulse frequency* or/and decreasing *workpiece rotating speed*, as per

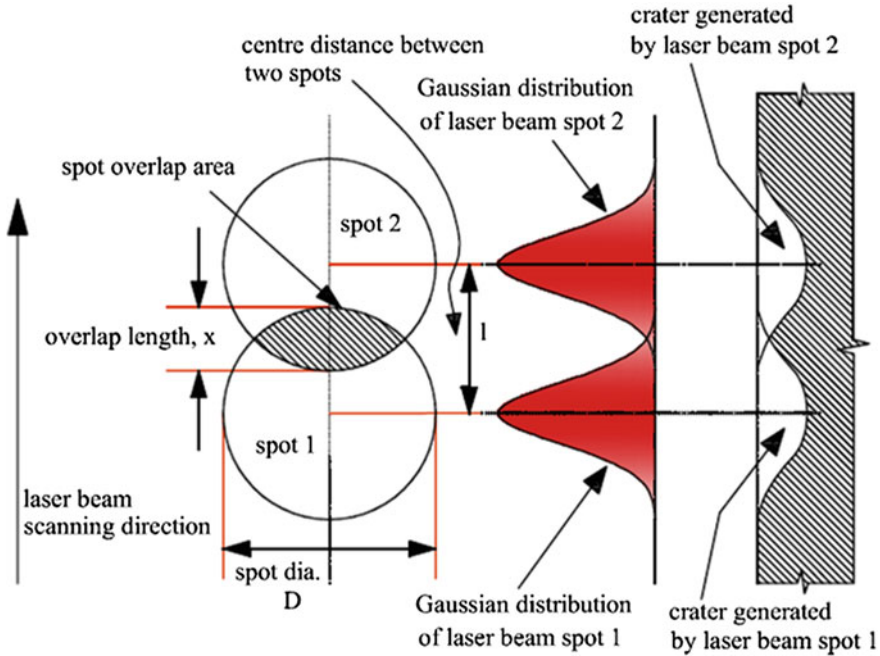


Fig. 1 Schematic view of overlap between consecutive spots showing Gaussian energy distribution (Kibria et al. 2012)

Eq. 3. Circumferential overlap percentage (CO_p) is another important criterion during laser micro-turning process. The relationship of this factor with laser process parameters can be formulated as follows.

The schematic view of *circumferential overlap* during laser beam scanning for two successive rotations is shown in Fig. 2. Let, N and D_s are the *rotating speed* in rpm and diameter of sample in mm, respectively. Now, the linear *scanning speed* of laser beam is, $v = \frac{\pi \times D_s \times N}{60}$ in mm/s. The circumferential length of sample is, $L = \pi \times D_s$. Now, the time taken by the laser beam to scan one complete rotation is, $t_s = \frac{L}{v} = \frac{60}{N}$ in seconds. If, the sample is moved through an *axial feed rate*, f (mm/s), then the movement of sample in t_s seconds is, $l_c = f \times t_s = \frac{60 \times f}{N}$ in mm. Therefore, from Fig. 1, the *circumferential overlap percentage* can be calculated from,

$$CO_p = \frac{\text{overlap length}}{\text{spot size}} = \frac{x_c}{D} = \left(1 - \frac{l_c}{D}\right) = \left(1 - \frac{60 \times f}{D \times N}\right) \times 100\% \quad (4)$$

In the above equation, x_c and D are laser scan overlap length (in mm) and laser spot diameter (in mm), respectively. In Fig. 2, it is observed that the two successive beam scans i.e. $(n - 1)$ th and n th produce an overlap length of x_c during rotation of workpiece and the workpiece moves l_c in its axial direction.

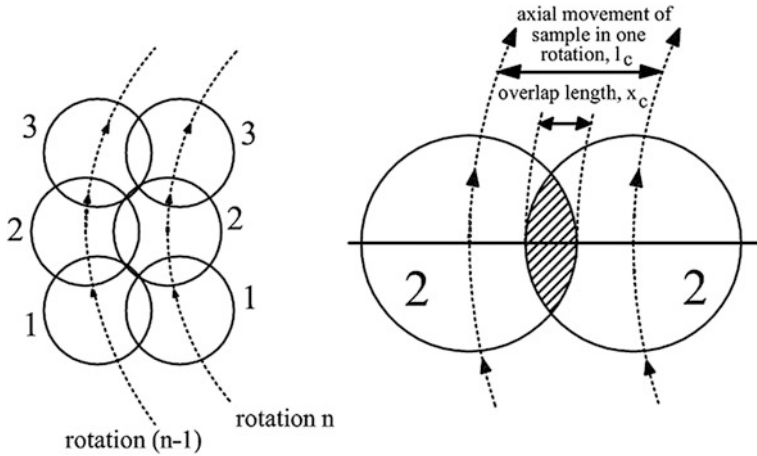


Fig. 2 Schematic representation of circumferential overlap between two consecutive rotations (Kibria et al. 2012)

It has already been said that for three dimensional laser beam machining, two intersecting laser beam sources are used (Chrysolouris et al. 1988). Each laser produces the corresponding blind cutting kerfs which converges and results in the solid stock removal from the machining zone. However, it is very difficult to remove thin layer from cylindrical shaped work surface. Experimental as well as theoretical research investigation into single and two dimensional laser beam machining of advanced ceramics like aluminum oxide, silicon nitride, silicon carbide, magnesia etc. have been conducted successfully by researchers across the globe (Samant and Dahotre 2008a, b; Dhupal et al. 2008). However, possibilities of micro-turning of these ceramics are in developing stage. Hence, extensive research is needed for developing laser materials processing technology for machining these advanced engineering materials with required geometrical shape and higher dimensional accuracy. To study and investigate the effect of various process parameters during laser micro-turning process, which removes very thin layer from work surface using single-laser beam and also to achieve desired surface profile on machined components, in the present investigation, laser micro-turning of cylindrical shaped alumina ceramic material by pulsed Nd:YAG laser have been performed based on various experimental schemes.

Figures 3a and b depict the schematic views for lower and higher values of *circumferential overlap* at high and low value of workpiece feed rate, respectively. From Fig. 3a, it is obvious that at low *circumferential overlap percentage*, the laser micro-turning surface is rendered with lots of micro-peaks, which cause higher surface roughness values. However, this generation of micro-peaks can be avoided at higher *circumferential overlap* values (as shown in Fig. 3b).

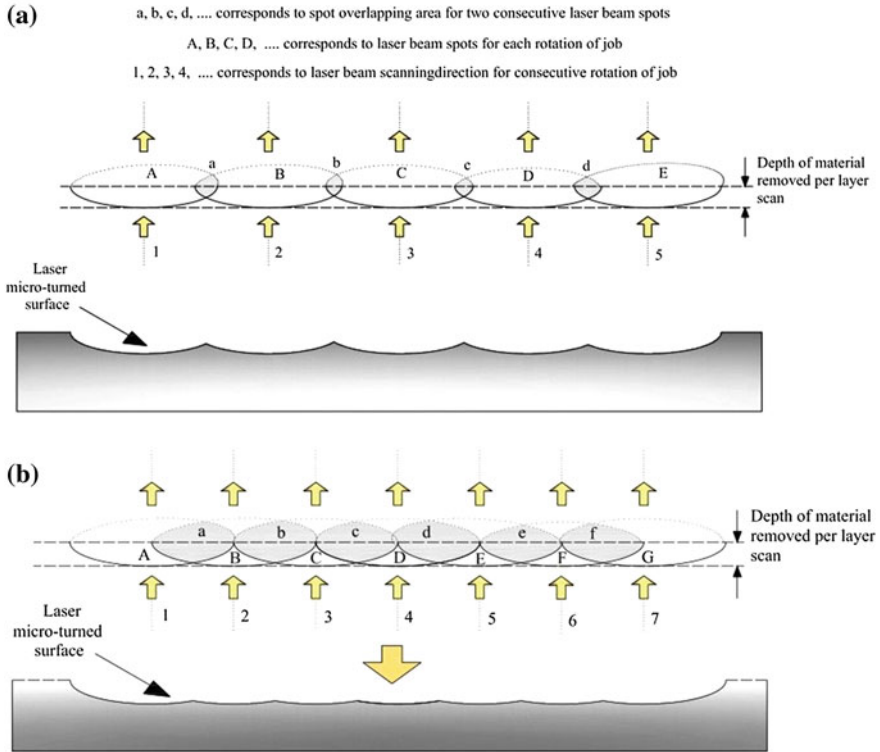


Fig. 3 Schematic view of laser micro-turned surface for (a) low and (b) high percentage of circumferential overlap for consecutive rotations (Kibria et al. 2013a)

3 Development of Laser Micro-turning System

To carryout laser micro-turning operation on cylindrical workpiece using the pulsed Nd:YAG laser set-up, a separate work holding and rotating unit has been developed indigenously. The complete work holding and rotating system consists of three components, (i) servomotor and developed workpiece holding fixture, (ii) servomotor amplifier, and (iii) power supply and interfacing unit. Figure 4 shows the complete schematic diagram of the developed workpiece rotating system. In Table 1, the specifications of the servomotor used for developing the workpiece rotating system are enlisted. A collet, which can grip cylindrical workpiece of diameter ranging from 2 to 16 mm, is mounted to the shaft of the servomotor very rigidly and accurately so that when the servomotor rotates in any desirable speed, it produces minimum amount of eccentricity due to rotation. The eccentricity of rotation was measured by using a dial gauge and the error was about 3 μm . The workpiece gripped with the collet can be rotated by the signals coming from servo amplifier at any rotational speed within the range of rotation of the servomotor.

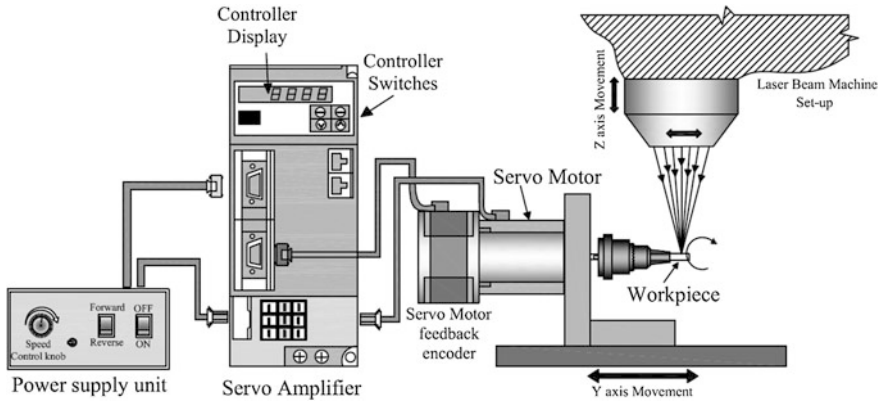


Fig. 4 Schematic representation of workpiece holding and rotating system (Kibria et al. 2012)

Table 1 Detailed specifications of servomotor used

Specifications	Description
Servomotor type	GYS101DC2-T2A
Input voltage	AC 200 V
Rated output	100 W
Rated speed	3000 rpm
Encoder	17-bit INC
Winding insulation class	IP67
Oil seal/shaft	Without an oil seal

The base of the fixture was made in such a dimension so that the whole fixture can be fixed by the slot provided on the X-Y worktable of the pulsed Nd:YAG laser system.

The speed of the servomotor was controlled using a servo amplifier. In Table 2, the detailed specifications of the servo amplifier are enlisted. The connections between the servomotor and servo amplifier are already shown in Fig. 4. The servo amplifier has four keys, (i) Mode change key (ii) Shift/Enter key (iii) Sub-mode selection key (UP) and (iv) Sub-mode selection key (DOWN). The amplifier has four-digit display. By systematic method and using the four keys, one can provide the input speed to the servo amplifier to get a particular rotational speed of the servomotor. Apart from the servomotor and servo amplifier, a power supply and

Table 2 Detailed specifications of servo amplifier

Specifications	Description
Amplifier type	RYC101D3-VVT2
Input voltage	Single-phase 200–230 V
Rated output	100 W
Circuit breaker	EA33AC/5

interfacing unit has been developed indigenously. The unit provides power to both the servomotor and servo amplifier. Moreover, there are some additional switches and knobs by which one can change the *rotating speed* of servomotor manually. In addition, the user can alter the rotational direction of servomotor by various switches. The power supply and interfacing unit gets power from the two-phase AC power supply line. The servomotor and its fixture is placed on the CNC X-Y worktable and by using CNC servo controller and personal computer system, feed is given along the axis to the rotating workpiece during laser micro-turning operation. After one pass of laser scan along the desired length of turning, the focusing lens was moved down by Z axis feed rate with the help of CNC controlled Z axis motion so as to focus the laser beam to the laser micro-turned surface generated by previous laser beam scanning. Thus, the desired depth and length of micro-turning surface is generated on cylindrical workpiece of a particular diameter.

4 Experimental Methodology of Laser Micro-turning

The entire experimentation was performed in a CNC controlled pulsed Nd:YAG laser system (manufactured by Sahajanand Laser Technology Ltd, India) as shown in Fig. 5. The beam of the system operates in Gaussian mode (TEM_{00}) and the wavelength of the beam is 1064 nm. The pulse duration of the laser beam is in the range of 120–150 ns. In the present pulsed Nd:YAG laser system, the polarization of the laser is random. The beam was focused to spot size of 100 μm (measurement of single spot on alumina workpiece surface) using a 50 mm focal length lens. The indigenously developed work holding and rotating fixture, which was manufactured

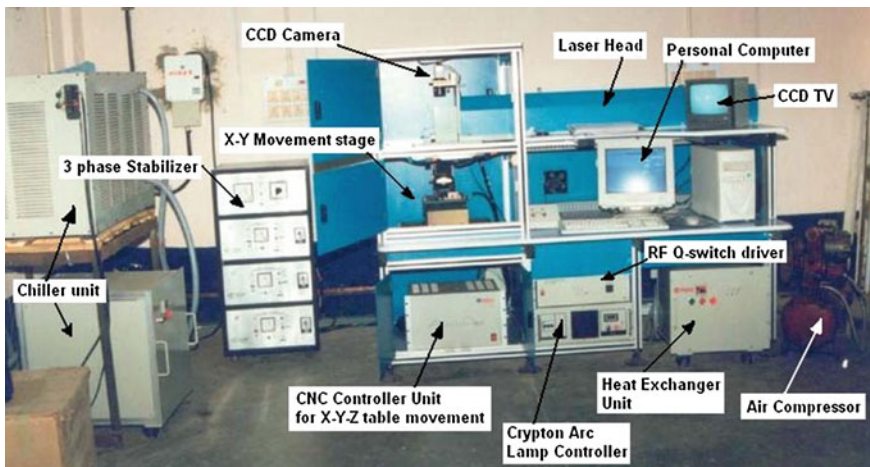


Fig. 5 Photographic view of the pulsed Nd:YAG laser machining system (Kibria et al. 2012)

Table 3 Major thermo physical properties of aluminium oxide ceramics

Properties	Values and units
Melting temperature	2050 °C
Creep rate	10^{-9} s^{-1} at 150 MPa
Density	3.984 g/cm ³
Specific heat	755 J/kg K
Activation energy	325(25) kJ/mol
Thermal conductivity	33 W/mK
Tensile strength	267 MPa
Thermal diffusivity	0.111 cm ² /s
Bulk modulus	257 GPa
Shear modulus	167 GPa
Grain size	5 μm

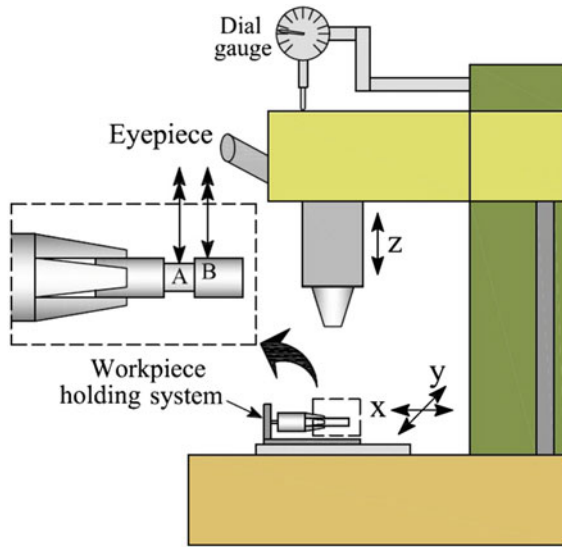
to facilitate the laser micro-turning operation, is used to hold and rotate the workpiece. A collet attached to the axis of the motor was used to grip the cylindrical work sample and the collet with the job was rotated through different speeds. Axial feed to the sample up to the desirable length of turn was provided by the Y directional feed rate of the CNC X-Y table operated by a personal computer attached to the Nd:YAG laser system. To encompass layer-by-layer removal of material from the cylindrical surface, after each scan of entire micro-turning surface, the focusing lens was moved down to provide the focal point to the previously machined micro-turning surface. Using the Multisawing software installed in the computer attached to pulsed Nd:YAG laser system, the length of micro-turning was selected as 5 mm. Moreover, the *Y feed rate* and *Z feed rate* was controlled by this software. Cylindrical shaped aluminium oxide ceramic (99 % pure) of size 10 mm in diameter and 40 mm in length was used as workpiece material. The major thermo and physical properties of aluminum oxide are enlisted in Table 3.

5 Various Measurement Schemes

Laser micro-turning experimentation was conducted at various experimental schemes. The process parameters involved during laser micro-turning operation were *laser average power*, *pulse frequency*, *workpiece rotational speed*, *assist air pressure* and *Y feed rate*. The *average power* of laser beam is measured using a laser power measuring device (make: Ophir Optronics Solutions Ltd, Israel). The laser power measuring device consists of power meter and the power sensor. To measure the *average power* of the laser beam, the sensor was kept at defocusing plane of laser beam and the power was directly noted from the digital display of the power meter.

After conducting each experiment at various parametric combinations, machining depth and surface roughness (Ra and Rt) was measured. The machining depth of the laser micro-turned surface was measured with the help of optical

Fig. 6 Scheme of micro-turning depth measurement using optical microscope



measuring microscope (Olympus STM6, minimum measurable dimension = $0.5 \mu\text{m}$) using a $10 \times$ magnification lens. The scheme of measurement of depth of cut using the optical measuring microscope is shown in Fig. 6. As shown in figure, at first, the lens of the microscope is focused onto the non-turned workpiece surface such as point B and then focused onto the micro-turned surface such as at point A. The values of these heights are measured by using a high precision dial gauge kept on the Z-axis stage of optical microscope. The result of these height difference measures the machining depth for the experiment. In experimental scheme, where depth deviation was selected as response criterion, the depth deviation was measured by simply differentiating the machining depth and target depth (taken as $100 \mu\text{m}$). The surface roughness (R_a and R_t) was measured along the axis of the cylindrical work sample by using SURFCOM 120A-TSK roughness measuring instrument. During roughness measurement, the cutoff length (λ_c) has been carefully chosen so that variations due to form errors are excluded and surface finish related to the closely spaced irregularities can be measured correctly. During roughness measurement, the cut-off length and total length of measurement were set as 0.25 and 2.5 mm, respectively.

6 Results and Discussion

Very few researches have been carried out in laser micro-turning process by the authors (Kibria et al. 2010b, 2013a, 2014a). Kibria et al. (2010b) have introduced the laser micro-turning operation as an advanced machining technology to machine

or micro-turn various hard-to-machine engineering ceramics. A very few research work have been carried out on micro-turning process of alumina (Al_2O_3) ceramic using pulsed Nd:YAG laser system. Authors have done basic experimental investigation describing the influence of *lamp current*, *scanning speed* and *pulse frequency* on surface roughness (Ra) and depth of cut. In the experimentation, surface roughness achieved was much higher i.e. in the range of 6.45–11.48 μm . Moreover, the depth of cut was in the range of 38 and 223 μm . This amount of fluctuations in the results of surface roughness and depth of cut reveals that process variables involved in laser micro-turning operation are dynamic in nature and process responses are significantly related with simultaneous variation of parameters during experiments. The same group of authors carried out experimental investigation on laser micro-turning process for machining various grades of Aluminum Oxide (Al_2O_3) ceramics (60, 80 and 99 % pure Al_2O_3 ceramics) to study the effects of various laser micro-turning process parameters on surface roughness (Ra) and depth deviation criteria (Kibria et al. 2014a). The same group of authors performed experimental study and multi-objective optimization during laser micro-turning process to machine 99 % pure Al_2O_3 ceramics using combined approach of Taguchi Methodology and Grey Relational Analysis (Kibria et al. 2013a). Experimentation and analysis have also been performed varying the significant process parameters revealed from Taguchi based experiments. All these experimentations deal with basic study of laser micro-turning process to search out the significant process parameters and their suitable working ranges. However for successful study and analysis of laser micro-turning process, *spot overlapping percentage* (SO_p) and *circumferential overlap percentage* (CO_p) play major roles. Moreover, for successful implementation of this novel process in various micro-engineering industries, surface roughness achieved as in (Kibria et al. 2010b, 2014a, 2013a) should be reduced by considering some novel machining strategies during laser micro-turning. The experimental results and analysis considering some novel machining strategies are shown and described hereafter.

6.1 Study the Influences of Overlap Factors on Surface Roughness Criterion

To study the effects of various percentages of *spot* as well as *circumferential overlap*, experiments have been conducted at various parametric combinations of process parameters, which are related to the overlap factors (Kibria et al. 2014b). A well-designed set of experiments has been performed to vary one factor at a time (OFAT) and surface roughness is measured. The levels and ranges of various parameters like *pulse frequency*, *workpiece rotating speed* and *Y feed rate* for achieving the *spot overlapping percentage* (SO_p) and *circumferential overlap percentage* (CO_p) is shown in Table 4. For each of the experiments, *the number of laser scan passes* was 100. In each of the workpiece, three experiments were

Table 4 Experimental conditions and ranges of process parameters (Kibria et al. 2014b)

Condition	Description
Average power, W	7, 8
Pulse frequency, Hz	3000, 4000, 5000, 6000, 7000
Workpiece rotating speed, rpm	200, 300, 400, 500, 600
Y feed rate, mm/s	0.1, 0.2, 0.3, 0.4, 0.5
Pulse width, % of duty cycle	variable
Air pressure, kgf/cm ²	1.3
Z feed rate, mm/s	0.01

conducted. During the experiments, surface roughness (Ra) was measured as the process criterion. A length of 5 mm was micro-turned on the cylindrical workpiece. In the present experimental study, the levels of two process parameters i.e. *pulse frequency* and *workpiece rotating speed* were chosen carefully so that the *spot overlapping percentages (SO_p)* of the successive laser spots have definite and positive values. In Fig. 7 shows the variation of *spot overlapping percentage* while varying *workpiece rotating speed* and *pulse frequency* values. Moreover, the *axial feed rate* or *Y feed rate* of work sample was chosen carefully so that its values compiled with *workpiece rotating speed* give positive values of *circumferential overlap percentages*. The variation of *circumferential overlapping percentage* at various parametric combinations of *Y feed rate* and *workpiece rotating speed* is shown in Fig. 8. These two plots have been drawn based on the considered range of all the related process parameters of *spot overlap* as well as *Circumferential overlap*. It is shown in both plots of *spot overlap* as well as *circumferential overlap percentage* that some points have been considered for negative overlap percentage to show the effect of the conditions of no overlap on surface roughness criterion.

Fig. 7 Variation of spot overlapping percentage at various workpiece rotating speed and pulse frequency

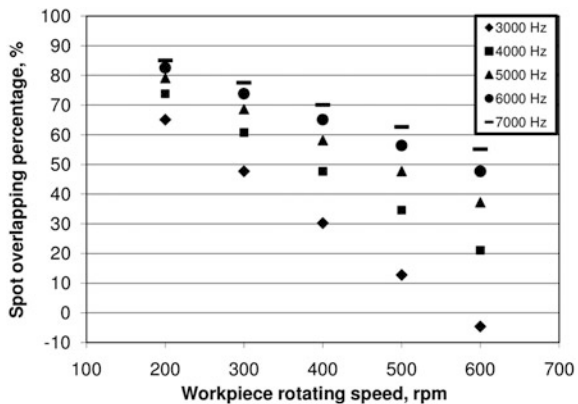
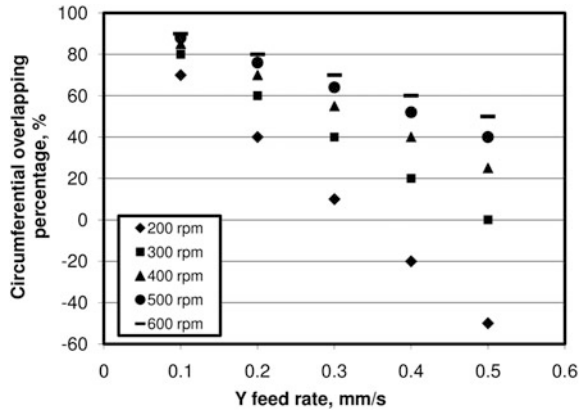


Fig. 8 Variation of circumferential overlapping percentage at various Y feed rate and workpiece rotating speed



6.1.1 Influence of Spot Overlap on Surface Roughness (Ra)

Each experiment was repeated three times and the average of three surface roughness values was taken to plot various graphs. Figures 9 and 10 show the variation of surface roughness (Ra) for varying *spot overlapping percentage* at different *pulse frequency* and *workpiece rotating speed*, respectively. It is already described that the *spot overlap percentage* can be varied by two methods, (i) by varying *workpiece rotating speed* keeping the *pulse frequency* at a constant value, and (ii) by varying *pulse frequency* keeping the *workpiece rotating speed* at constant value. For the results shown in Fig. 9, the *average power* and *Y feed rate* were kept constant as 7 W and 0.3 mm/s, respectively. From this figure, it is observed that roughness of the micro-turned surface reduces with the increase of *spot overlap* for each of the *pulse frequency* settings. From Eq. 3, it is obvious that the reduction in *workpiece rotating speed* results in high overlap value between successive laser spots. This high amount of overlap results in even machined surface and reduces the

Fig. 9 Effect of spot overlapping on surface roughness (Ra) at different pulse frequency (Kibria et al. 2014b)

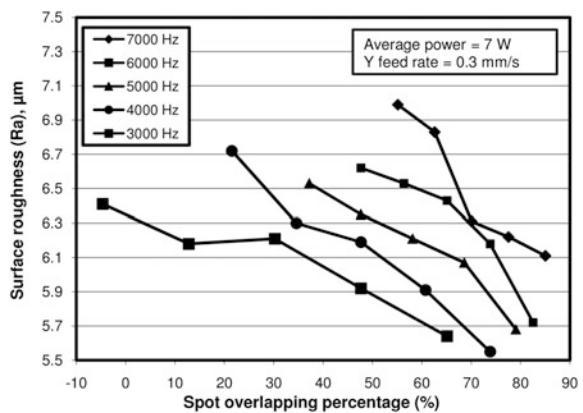
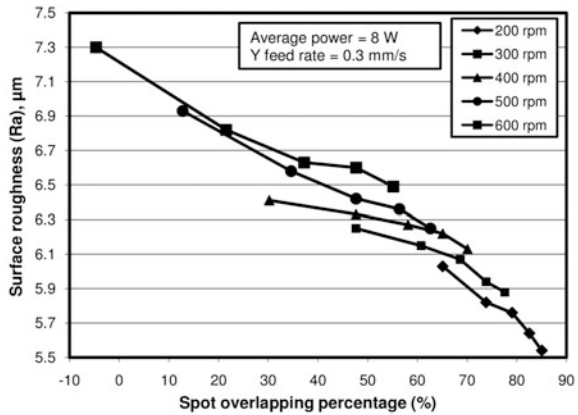


Fig. 10 Effect of spot overlapping on surface roughness (Ra) at different rotating speed (Kibria et al. 2014b)



surface roughness. It is also seen from the same plot that the surface roughness value increases with *pulse frequency* at any particular *spot overlap percentage* value. With the increase of *pulse frequency*, according to Eq. 3, the *spot overlap percentage* increases. However, at high *pulse frequency* condition, the time duration between two successive pulses is very less. Therefore, the material at the focused zone on the sample gets adequate thermal energy for melting and vaporization instantly. Thus, ultimately, the total amount of irradiated laser beam energy is high enough and it results in more depth of crater formed on the surface, which results higher value of surface roughness.

For the experimental results shown in Fig. 10, the *average power* and *Y feed rate* were kept constant at 8 W and 0.3 mm/s, respectively. The figure clearly indicates that with the increase of *spot overlap percentage* for any constant value of *workpiece rotating speed*, surface roughness (Ra) decreases. Due to high *percentage of spot overlap*, the material removal from the workpiece surface occurs uniformly and therefore, high quality machining surface is achieved. Furthermore, for same *spot overlap percentage* value, the micro-turned roughness is more for higher value of *workpiece rotating speed*. At higher setting of *workpiece rotating speed*, consecutive *spot overlap* is less, resulting uneven micro-turning surface.

6.1.2 Influence of Circumferential Overlap on Surface Roughness (Ra)

In Figs. 11 and 12, the effect of varying *circumferential overlap* values on surface roughness (Ra) is shown at different *Y feed rate* and *workpiece rotating speed*, respectively. In Fig. 11, the surface roughness has been plotted keeping *average power* at 8 W and *laser pulse frequency* at 5000 Hz. From Eq. 4, it is obvious that the *circumferential overlap percentage* mainly depends onto two process parameters i.e. *Y feed rate* and *workpiece rotational speed*. It is clear from this plot that the increase in *circumferential overlap percentages* i.e. increase in *workpiece rotating speed* with constant *Y feed rate* setting results in slight decrease in surface

Fig. 11 Effect of circumferential overlapping on surface roughness (Ra) at different Y feed rate (Kibria et al. 2014b)

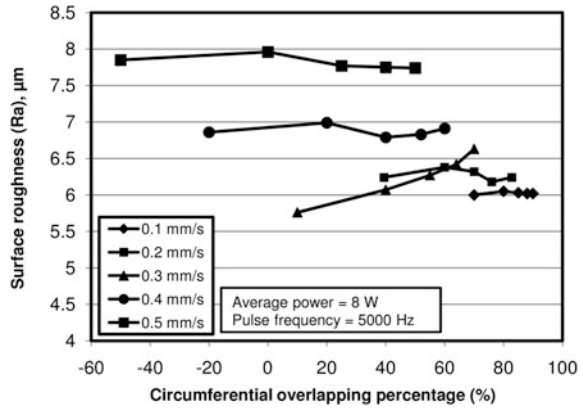
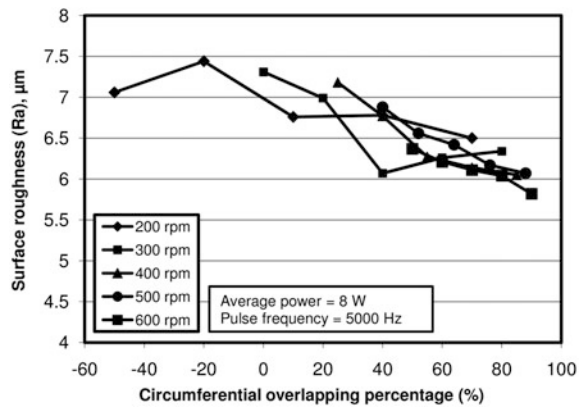


Fig. 12 Effect of circumferential overlapping on surface roughness (Ra) at different rotating speed (Kibria et al. 2014b)



roughness values. From Eq. 4, it is clear that *circumferential overlap percentage* increases with increasing *workpiece rotating speed* and this phenomenon has directly resulted for reduction of roughness of laser micro-turned surface. High *circumferential overlap percentage* results in uniform removal of material from laser irradiated surface and high finish surface is achieved. Moreover, it is also clearly seen from Fig. 11 that for a constant value of *circumferential overlap*, the increase in *Y feed rate* results in rougher micro-turned surface. Increase in *Y feed rate* of sample is resulted more null and void spacing between two successive scan widths and this phenomenon consequently results uneven and rough micro-turning surface.

In Fig. 12, the influence of *circumferential overlap* on surface roughness is shown at *average power* of 8 W and *pulse frequency* of 5000 Hz, respectively. It is observed from this plot that with the increase in *circumferential overlap*, roughness of the machined surface decreases for each *workpiece rotating speed* setting. Due to high *circumferential overlap*, the laser scan widths for successive rotation of workpiece come closer to each other and in turn, this phenomenon results in even

and regular micro-turning surface. It shows that at higher *workpiece rotating speed* settings, the amount of *circumferential overlap* is high and further it results lower value of surface roughness of the surface profile produced during laser micro-turning operation.

6.1.3 Microscopic Analysis of Laser Micro-turned Surface

Studies of scanning electron microscopy (SEM) micrographs of the laser micro-turned surface have also been conducted to get a clear picture of the effect for varying the laser micro-turning process parameters. Figure 13a–d show and compare the micro-turned surface characteristics for different *spot overlap* and *circumferential overlap* values, accounted for varying the related process parameters i.e. *workpiece rotating speed*, *laser pulse frequency* and *Y feed rate* of workpiece. Comparing the experimental parametric settings and SEM micrographs in Fig. 13a and b, it is seen that with increased *spot overlap percentage* from 21.43 to 73.81 %, due to increase in *pulse frequency* from 4000 to 6000 Hz and decrease in *workpiece rotating speed* from 600 to 300 rpm, the Ra value of micro-turned surface is reduced from 6.72 to 6.18 μm . From Fig. 13c and d, it is observed that when the *circumferential overlap percentage* is increased from 25 to 90 % by reducing the Y

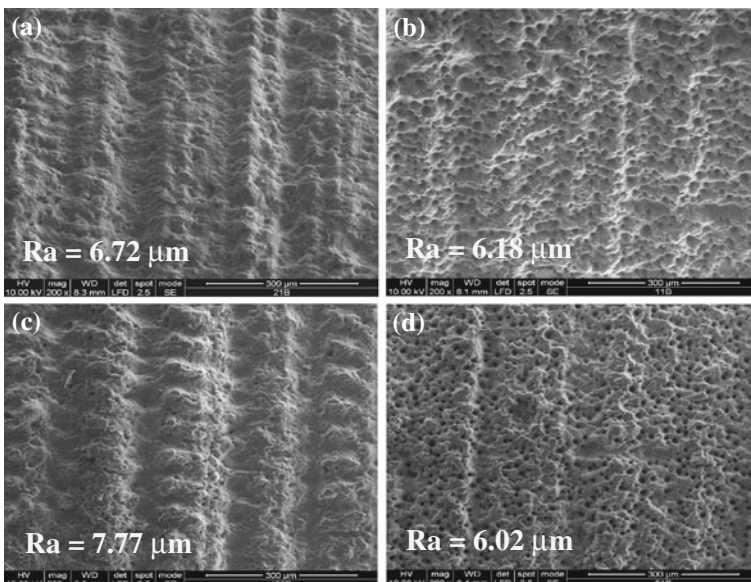


Fig. 13 SEM micrographs of the laser micro-turned surface of work samples machined at parametric combinations of average power, pulse frequency, workpiece rotating speed and Y feed rate of (a) 7 W/4000 Hz/600 rpm/0.3 mm/s, (b) 7 W/6000 Hz/300 rpm/0.3 mm/s, (c) 8 W/5000 Hz/400 rpm/0.5 mm/s and (d) 8 W/5000 Hz/600 rpm/0.1 mm/s (Kibria et al. 2014b)

feed rate from 0.5 to 0.1 mm/s and increasing the workpiece rotating speed from 400 to 600 rpm simultaneously, quite uniform micro-turning surface was realized. Ra value is reduced from 7.77 to 6.02 μm .

6.2 Study of Defocusing Conditions at Multi-objective Optimization to Achieve Better Quality Surface

Response surface methodology (RSM) based approach has been considered to carry out micro-turning operation of cylindrical shaped alumina ceramic (Kibria et al. 2012, 2013b). A lot of pilot experiments have been conducted before selecting the actual process parametric ranges. Five levels of each process parameters i.e. average power, pulse frequency, workpiece rotational speed, air pressure, Y feed rate were considered as shown in Table 5. The experimentation has been carried out based on central composite rotatable second-order design (CCRD). After each experiment, surface roughness (Ra) and micro-turning depth deviation have been measured. The measurement scheme of surface roughness and machining depth are already discussed in previous sections. The target machining depth was taken as 100 μm . The deviation in depth was calculated according to the following equation (Kibria et al. 2013b).

$$Y_{\text{depth dev.}} = Y_{td} - Y_{md} \quad (5)$$

where, $Y_{\text{depth dev.}}$ is the amount of depth deviation, Y_{td} is the targeted depth and Y_{md} is the machined depth accounted during experiments. MINITAB™ statistical software was used to develop the design of matrix of experimentation and further analysis of obtained values of responses from measurement schemes. Multi-objective optimal parametric combination of process variables has been obtained for achieving least values of responses i.e. surface roughness and depth deviation. To achieve further high quality machined surface, machining was done at various defocusing conditions of laser beam and also by varying the number of laser scan passes. Other process parameters were kept constant at optimal parametric combination obtained in multi-objective optimization.

Table 5 Factors and various levels of the process parameters for RSM experimentation (Kibria et al. 2013b)

Parameters	Unit	Levels				
		-2	-1	0	1	2
Average power	W	6	7	8	9	10
Pulse frequency	Hz	3000	4000	5000	6000	7000
Rotational speed	rpm	200	300	400	500	600
Air pressure	kgf/cm ²	0.3	0.8	1.3	1.8	2.3
Y feed rate	mm/s	0.1	0.2	0.3	0.4	0.5

6.2.1 Multi-objective Optimization of Surface Roughness and Depth Deviation

To achieve the targeted shape as well as machined surface during laser micro-turning operation considering the performance criteria, multi objective optimization has been performed (Kibria et al. 2013b). Figure 14 shows the multi response optimization result during laser micro-turning operation of alumina ceramic with pulsed Nd:YAG laser system. In the mentioned figure, columns of the plot represents each parameter with their ranges considered and each row of the plot represents the performance criteria measured in this experimentation. Moreover, each cell shows how the process criteria changes as function of one of the process parameters while keeping the other parameters fixed. From this figure, it can be seen that the parametric combination for multi-objective optimization i.e. minimization of all the process responses was achieved as *average power* of 7.81 W, *pulse frequency* of 5601.59 Hz, *workpiece rotational speed* of 435.60 rpm, *air pressure* of 0.30 kgf/cm² and *Y feed rate* of 0.4434 mm/s. During multi-objective optimization, all the responses were optimized with composite desirability (D) value of 1. Due to the constraints of the existing machine settings, the parameters values were taken nearer to the value obtained during optimization. Experimentation has been conducted nearer the feasible setting of process parameters achieved during multi-objective optimization to evaluate the actual process criteria values. The percentage error of experimental results for the optimized responses were compared with RSM based estimated results as obtained from developed empirical models and the results are tabulated in Table 6. The percentage errors calculated are within acceptable range (<5 %). This shows a good agreement of the optimized responses at the optimal parameters setting during laser micro-turning of alumina ceramic.

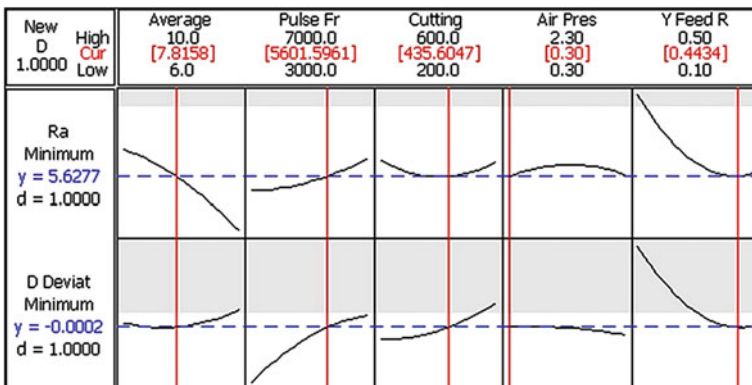


Fig. 14 Multi objective optimization results for surface roughness (Ra) and depth deviation (Kibria et al. 2014b)

Table 6 Comparison of experimental and RSM estimated results at optimal parametric combination (Kibria et al. 2013b)

Optimization	Experimental parameters settings			Responses	Experimental results	RSM estimated results	Percentage of error (%)
	Parameters	Unit	Value				
Multi-objective optimization	Average power	W	7.81	Surface roughness, Ra depth deviation	5.91 μm -0.00021 mm	5.63 μm -0.00020 mm	4.78 4.76
	Pulse frequency	Hz	5600				
	Rotating speed	rpm	436				
	Air pressure	kgf/cm ²	0.30				
	Y feed rate	mm/s	0.443				

6.2.2 Study of Laser Defocusing Conditions During Laser Micro-turning

Although, surface roughness has been considered as minimum is the best type response, the value of optimal surface roughness is quite high (i.e. 5.63 μm in RSM and 5.91 μm in validation). This amount of roughness may be due to generation of micro-peaks on the machined surface. However, in actual practice, to produce an acceptable machined surface and to manufacture durable and reliable products, which can provide high-end performances, the roughness of machined surface should be lowered down further. Therefore, it is felt that further experiments should be carried out to minimize the surface roughness values without impeding the depth deviation value. Therefore, to further improve the quality of machined surface and to reduce the laser micro-turned surface roughness, experiments have been conducted at RSM based multi-objective optimization setting as shown in Table 6 (Kibria et al. 2015). Two process parameters i.e. *defocusing position* and *number of laser scan pass* were varied during defocused laser micro-turn machining. Figure 15 shows the process mechanism of laser defocused laser micro-turning operation. The optimal machined surface has lots of micro-peaks and by further machining at various defocusing conditions and several laser beam scan passes, these micro-peaks can be removed by lowering the laser beam energy density through melting and vaporization of material from these micro-peaks. A lot of pilot experiments have been conducted to select the range of defocusing planes in which the workpiece surface to be kept and rotated during machining operation. The defocus position is termed as upward when the laser focus point is above the workpiece surface, whereas defocus position is called as downward when the laser focus point is inside the workpiece or below the surface to be machined. The values of defocus positions considered in the present experimentation are shown in Table 7. At each defocusing planes, experiments have been carried out by varying the number of laser scans. Here, surface roughness, R_t has been considered as additional response to study the laser micro-turning surface features in more details.

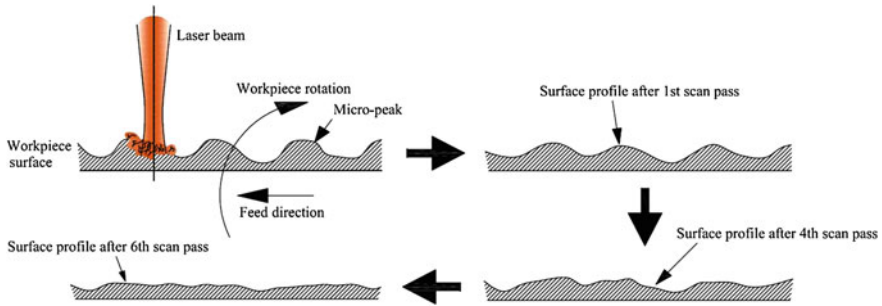


Fig. 15 Process of removal of micro-peaks during defocused laser micro-turning process (Kibria et al. 2013c)

Table 7 Factors and various levels for further experimentation (Kibria et al. 2013c)

Parameters	Unit	Levels	
Defocus position	mm	Upward	Downward
		-0.2, -0.4, -0.6, -0.8	+0.2, +0.4, +0.6, +0.8
Number of passes	-	1, 2, 3, 4, 5, 6, 7, 8, 9, 10	

This response of surface roughness is much responsive to the high peaks or deep scratches on the surface of assessment. It is defined as the vertical measurement of distance between the highest peak and the lowest valley within the assessment length of surface profile. It is the summation of maximum height of peak from mean line (Rp) and maximum depth of valleys from mean line (Rv) of the surface profile (Gadelmawla et al. 2002). Although, the present set of experiments have been conducted to further reduce the surface roughness (Ra and Rt) criteria through various experiments of varying the focal positions and number of laser beam passes, as it is basically a laser micro-turning operation, therefore, the dimensional accuracy features of the machined parts or components would be worsen, mainly the depth deviation of micro-turning surface. The depth deviation of the machined parts has been measured after conducting each two consecutive laser beam passes. After each experiment, the surface roughness (Ra and Rt) and depth deviation of the machined surface were measured by same technique as discussed in measurement schemes. The depth deviation is measured using the following equation (Kibria et al. 2015).

$$Depth\ deviation = Machined\ depth - Machined\ depth\ achieved\ at\ optimal\ setting \tag{6}$$

Based on the obtained results of responses i.e. surface roughness (Ra and Rt), various plots have been drawn and shown in Figs. 16, 17, 18 and 19. In Fig. 16, the effect of number of laser scan passes on surface roughness (Ra) is shown at various upward defocusing positions. The other process parameters were kept constant at

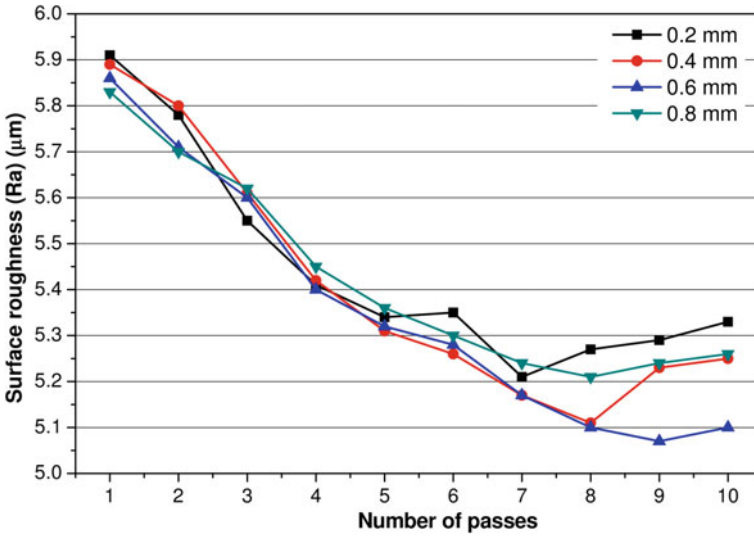


Fig. 16 Variation of surface roughness (Ra) with number of laser scan passes at various upward defocus positions (Kibria et al. 2013c)

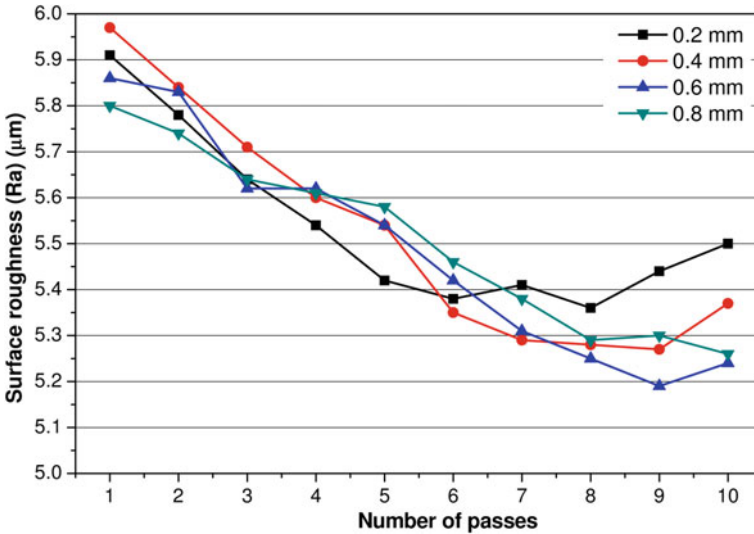


Fig. 17 Variation of surface roughness (Ra) with number of laser scan passes at various downward defocus positions (Kibria et al. 2013c)

7.81 W/5600 Hz/436 rpm/0.30 kgf-cm⁻²/0.443 mm/s of average power, pulse frequency, workpiece rotating speed, assist air pressure and Y feed rate, respectively. In Fig. 16, it is observed that surface roughness of laser micro-turning

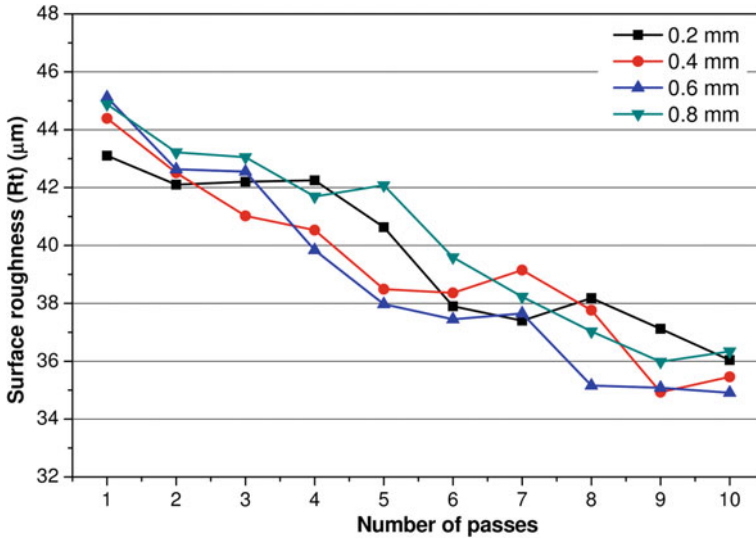


Fig. 18 Variation of surface roughness (Rt) with number of laser scan passes at various upward defocus positions (Kibria et al. 2013c)

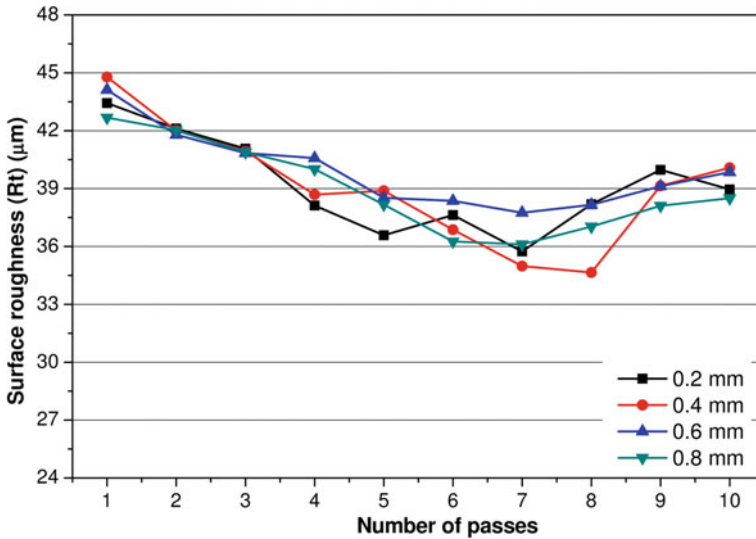


Fig. 19 Variation of surface roughness (Rt) with number of laser scan passes at various downward defocus positions (Kibria et al. 2013c)

surface is decreasing with the increase in *number of laser beam passes* at each setting of *downward defocusing positions*, i.e. 0.2, 0.4, 0.6 and 0.8 mm. During machining in defocusing conditions, with the increase of *number of laser scan*

passes, the height of various micro-sized peaks on the machining surface reduces due to melting and evaporation of material from micro-peaks and therefore, the quality of the laser micro-turning surface is improved. The figure also depicts that at various defocus positions, different values of surface roughness are achieved for any particular *number of laser passes*. However, with the increase of defocus position, surface roughness of the laser turning surface is decreasing due to adequate laser beam energy, which removes the rough and irregular peaks from the workpiece surface and makes the surface even. Conversely, it is also observed that at higher value of defocus condition, i.e. at 0.8 mm, the roughness is much higher than 0.4 and 0.6 mm defocus positions. It is so because at 0.8 mm position, the energy density of the laser beam on the workpiece surface is very low and this amount of energy is unable to remove the micro-peaks from the laser micro-turned surface. These phenomena result in higher amount of surface roughness of the machined surface.

The effects of variation of *number of laser scan passes* on surface roughness (Ra) criterion is shown in Fig. 17 at various *downward defocusing positions*. During these experiments, the other process parameters were kept constant at 7.81 W/5600 Hz/436 rpm/0.30 kgf-cm⁻²/0.443 mm/s of *average power, pulse frequency, workpiece rotating speed, assist air pressure* and *Y feed rate*, respectively. From this plot, it is obvious that the *number of laser scan passes* has significant effect on surface roughness (Ra) criteria. The surface roughness value decreases with the increase in *number of laser beam passes* at each of the defocus positions. It is due to the removal of sharp micro-sized peaks from the workpiece surface by the irradiated laser beam. However, after a certain *number of laser beam passes*, the surface roughness increases to a little extent for each of the focusing conditions. This is because, after certain *number of passes*, the removal of material from workpiece surface is not uniform and due to the high intense laser beam, the machined surface achieved is irregular and uneven. At higher setting of *downward defocusing position* i.e. at 0.8 mm, the laser beam spot size is much high and correspondingly the energy density on the workpiece surface is very low. This low energy beam is rather incapable to remove the micro-sized peaks from the rough workpiece surface. Therefore, at higher value of *defocusing position*, the surface roughness is low compared to other defocusing conditions i.e. 0.4 and 0.6 mm.

Figure 18 shows the effect of varying the number of laser scan passes on surface roughness (Rt) at various *upward defocusing positions*. The other process parameters were kept constant at 7.81 W/5600 Hz/436 rpm/0.30 kgf-cm⁻²/0.443 mm/s of *average power, pulse frequency, workpiece rotating speed, assist air pressure* and *Y feed rate*, respectively. It is observed from this plot that the surface roughness (Rt) decreases with the increase in *number of laser scan passes* for all the settings of *defocusing positions*. It is due to the removal of micro-sized peaks from the rough laser micro-turning surface by the irradiated laser beam. From this figure, it is also observed that at same *number of laser beam passes*, lower setting of *defocusing position* results in higher value of surface roughness (Rt) compared to higher setting of *defocus positions*. This is mainly due to differentiation of energy densities at various focal positions and requirement of amount of laser beam energy to reduce

the height of micro-peaks. However, at 0.8 mm defocusing condition, the surface roughness (Rt) is high compared to 0.6 and 0.4 mm defocus conditions. This is because at 0.8 mm *defocusing position*, the energy density of laser beam is very low, which is unable to remove or reduce the micron-sized peaks from the work-piece surface.

The effect of variation of *number of laser scan passes* on surface roughness (Rt) value is illustrated in Fig. 19, while machining at various *downward defocusing positions*. The other process parameters were kept constant at 7.81 W/5600 Hz/436 rpm/0.30 kgf-cm⁻²/0.443 mm/s of *average power, pulse frequency, workpiece rotating speed, assist air pressure* and *Y feed rate*, respectively. The plot shows that with the increase in *number of laser scan passes* results in decrease of surface roughness (Rt) values up to a certain *number of passes*. With the increase of *number of passes* of laser beam, the overall heights of the uneven peaks on the laser micro-turned surface decreases. However, after certain *number of passes*, the roughness of micro-turning surface does not significantly vary. In some defocusing conditions such as 0.4 and 0.8 mm, the surface roughness increases after 7th *number of passes*. It is due to generation of small sized uneven peaks again on the laser micro-turned surface. The plot also shows that effect of *defocusing positions* on surface roughness criterion is very random. The minimum surface roughness is achieved at 0.4 mm defocus position and at 8th *number of laser beam passes*. At high defocusing condition, the laser beam energy density is very low and this amount of energy density is incapable of removing further micro-peaks from the rough and uneven surface of the workpiece.

It has been observed from various plots of surface roughness (Ra and Rt) that with the increase of *number of laser beam passes*, the surface roughness (Ra and Rt) decreases at all settings of upward defocus positions. However, at the same settings of *downward defocus positions*, the surface roughness (Ra) is having a trend of decreasing, whereas Rt is moderately varying with *number of laser beam passes* during the machining process. From various test results of the present set of experiments, the individual parametric combinations have been identified for achieving minimum values of individual responses and enlisted in Table 8. At 0.6 mm *upward defocus position* and 9th *number of laser beam passes*, the surface

Table 8 Parametric combinations to achieve minimum surface roughness (Ra and Rt) (Kibria et al. 2013c)

Responses	Parametric combination of average power, pulse frequency, workpiece rotating speed, air pressure and Y feed rate	Parametric setting of additional parameters		Minimum value of responses	
		Number of passes	Defocusing position	Surface roughness, Ra	Surface roughness, Rt
Surface roughness, (Ra, Rt)	7.81 W/5600 Hz/436 rpm/0.30 kgf-cm ⁻² /0.443 mm/s	9	0.6 mm (upward)	5.07 μm	35.08 μm
		8	0.4 mm (downward)	5.28 μm	34.65 μm

roughness (Ra and Rt) values are 5.07 and 35.08 μm , which is the smallest value. However, surface roughness, Rt is achieved as minimum as 34.65 μm (Ra = 5.28 μm) at defocus position of 0.4 mm downward and at 8th *number of laser beam passes*. Moreover, it is found from various test results that depth deviation of the laser micro-turned surface increases with the increase in *number of laser beam passes* for all the settings of *defocusing positions*. It is due to reduction of the overall height of the small-sized peaks on the laser turning surface. With lower setting of defocus value, higher value of depth deviation is achieved. With the increase in defocus length, the beam energy density decreases due to increase in laser beam spot size.

6.2.3 Analysis Based on SEM Micrographs of Laser Micro-turned Surface

To study the laser micro-turned machined surface comparatively, the microscopic analysis of the micro-turned surfaces machined at various parametric combinations also been analysed to get a clear picture of the effect of laser beam *defocusing positions* and *number of laser passes* during experiments. Figure 20a–f show SEM images (different magnifications) of the laser micro-turned surface machined at 0.2 mm *downward defocusing* after 10th passes (Ra = 5.50 μm , Rt = 38.96 μm), 0.8 mm *upward defocusing* after 10th passes (Ra = 5.26 μm , Rt = 36.34 μm) and 0.6 mm *upward defocusing* after 10th passes (Ra = 5.10 μm , Rt = 34.91 μm) of laser beam. Comparing these SEM images as well as surface roughness values, it is obvious that the quality of micro-turned surface machined at 0.6 mm *upward defocus position* and 10th *number of laser beam passes* is high compared to the machined surface shown in Fig. 20d and f.

The high magnification SEM images of the laser micro-turned surfaces machined at above-mentioned parametric combinations are shown in Fig. 21a–c, respectively. In Fig. 21a, it is seen that still the machined surface has some micro-peaks after machining at *defocusing position* of 0.2 mm and 10th *number of laser beam passes*. However, it is seen in Fig. 21b, there is no such micro-peaks on the machined surface. Because of irradiation of defocused laser beam on the surface, the micro-peaks melted as well as evaporated and some melted materials resolidified on the machined surface. On the other hand, the SEM image of the machined surface shown in Fig. 21c has no such micro-peaks as well as resolidified materials because of adequate laser beam energy irradiated on the material surface to completely evaporate and remove the micro-peaks from alumina surface.

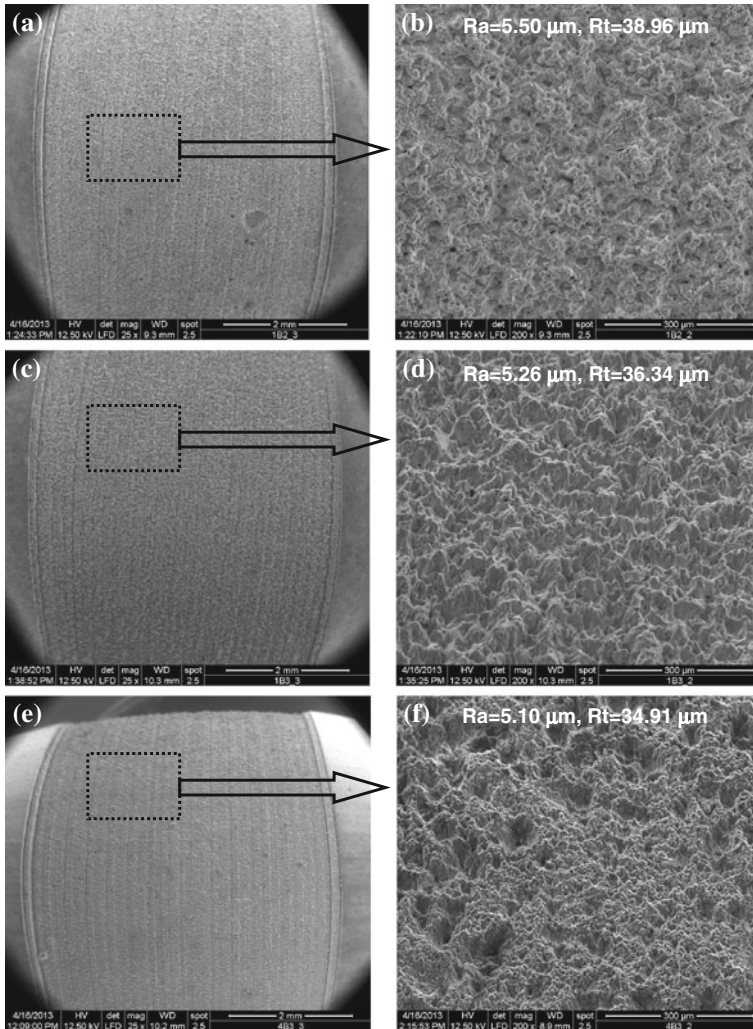


Fig. 20 SEM micrographs of laser micro-turned surface of alumina ceramic machined at 0.2 mm downward/10th pass (a and b), 0.8 mm upward/10th pass (c and d), and 0.6 mm upward/10th pass (e and f) of defocusing position and number of passes of laser beam

6.3 Comparative Study of Surface Roughness Criteria at Laser Focused and Defocused Conditions During Laser Micro-turning

In this experimental scheme, comparative investigation and analysis is carried out at focused and defocused conditions of laser beam during laser micro-turning process of aluminium oxide (Al_2O_3) ceramics to explore the effects of various process

Fig. 21 High magnification SEM micrographs of laser micro-turned surface machined at (a) 0.2 mm downward/10th pass, (b) 0.8 mm upward/10th pass and (c) 0.6 mm upward/10th pass of defocusing position and number of passes of laser beam

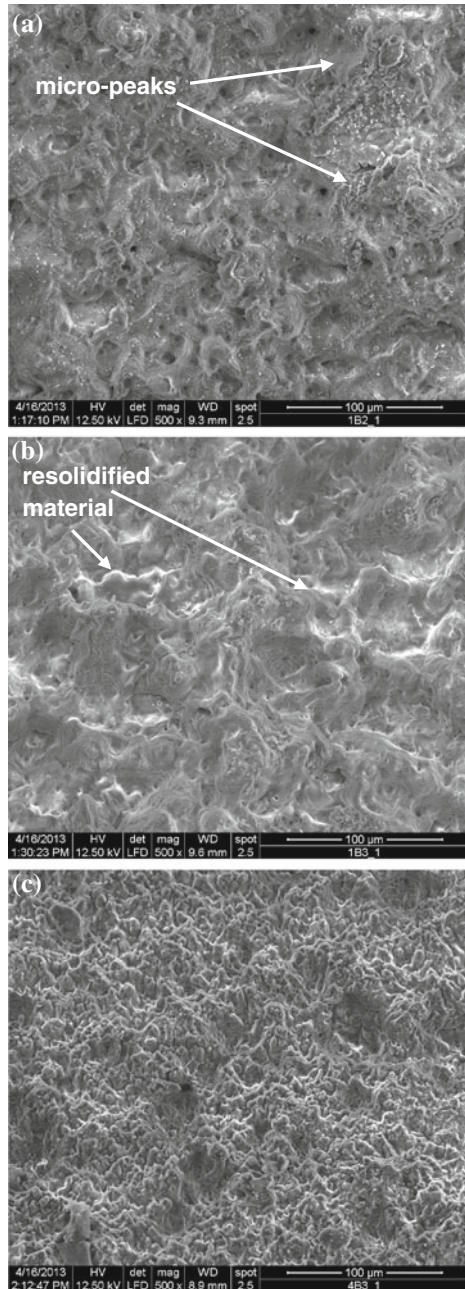


Table 9 Process parameters levels and other machining conditions

Variable parameters	
Process parameters	Levels
Average power	5, 6, 7, 8, 9, 10 W
Pulse frequency	4000, 4500, 5000, 5500, 6000 Hz
Rotational speed	200, 300, 400, 500, 600 rpm
Y feed rate	0.2, 0.3, 0.4, 0.5, 0.6 mm/s
Condition of lens	Focused, defocused
Defocused	0.2, 0.4, 0.6 mm upward
Constant parameters	
Air pressure	0.3 kgf/cm ²
Mode of operation	Q-switched (pulsed)
Type of Q-switch	Acousto optic
Mirror reflectivity	Rear mirror–100 % Front mirror–80 %
Beam diameter $1/e^2$	1 mm
Laser beam spot diameter	100 μ m

parameters such as *average power*, *pulse frequency*, *workpiece rotating speed* and *Y feed rate*. The experiments have been conducted utilizing one factor at a time (OFAT) experimental scheme. The target depth was set at 100 μ m. Table 9 shows the levels of process parameters considered. The table also shows the other process parameters which were kept constant during experimentation. In the previous experimentation, it is revealed that least surface roughness (Ra) is achieved as 5.07 μ m at 0.6 mm *upward defocusing condition*. Therefore, all the experiments in the present experimental scheme are carried out at various *upward defocused* and as well as *focused conditions*. After each experiment, surface roughness (Ra and Rt) has been measured.

Based on the results of surface roughness (Ra and Rt) values measured both the machining conditions i.e. focused and defocused, various plots are drawn and analysed in details hereunder. In Fig. 22, the effect of *average power* on surface roughness (Ra) is shown at focused and various upward defocusing conditions. The other process parameters were kept constant at *pulse frequency* of 5000 Hz, *workpiece rotating speed* of 400 rpm and *Y feed rate* of 0.4 mm/s. From this plot, it is observed that low value setting of *average power* results in high surface finish due to a smaller amount of melting and/or ablation of materials from work sample. As *average power* increases, the roughness of micro-turning surface also increases. It is also seen from the same plot that surface roughness values are less when laser micro-turning is carried out in *defocused conditions* compared to focus condition machining. In *defocus machining condition*, the energy density of laser beam is low, therefore, material from top surface micro-peaks is removed through melting and evaporation and surface conditions of machined surface is improved. The figure

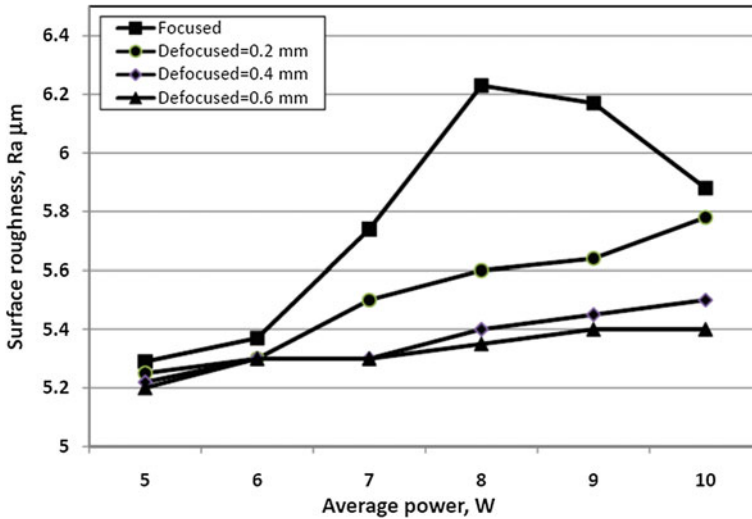


Fig. 22 Variation of surface roughness (Ra) with average power at focused and various upward defocus conditions

also depicts that at various *defocus positions*, different values of surface roughness are achieved for any particular *average power* value. With the increase of defocus position, surface roughness of the laser turning surface is decreasing due to adequate laser beam energy, which removes the rough and irregular peaks from the workpiece surface and makes the surface even.

Figure 23 shows the effect of *pulse frequency* on surface roughness (Ra) at *focused* and various *upward* defocusing conditions. The other process parameters were kept constant at *average power* of 8 W, *workpiece rotating speed* of 400 rpm and *Y feed rate* of 0.4 mm/s. It is evident from this plot that surface roughness (Ra) slightly increases at *focused* and other *defocused* conditions. According to the Eq. 7, it is clear that with the increase of *pulse frequency*, *peak power* of laser beam decreases (Kibria et al. 2013b). However, the time interval between two consecutive pulses of laser beam is very small, therefore the top surface of the workpiece gets adequate energy to melt and vaporize rapidly and it results in more peaks and valleys on the micro-turned surface.

$$Peak\ power\ (P_P) = \frac{Average\ power\ (P_A)}{Pulse\ frequency\ (F_P) \times Pulse\ duration\ (\mu)} \quad (7)$$

It is also seen in the same plot that the values of surface roughness (Ra) is less at all parametric combinations during machining at all *defocus conditions* compared to machining at *focused condition*. It is due to adequate thermal energy consumed by the workpiece surface and as a result of this, the height of micro-peaks is less. The surface roughness values are less at higher *defocused machining conditions* i.e.

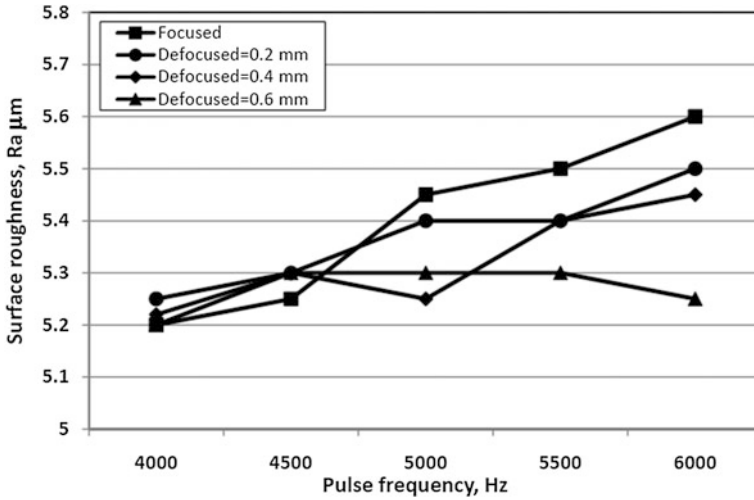


Fig. 23 Variation of surface roughness (Ra) with pulse frequency at focused and various upward defocus conditions

more defocused, more quality surface and it is due to adequate laser power density at laser material interaction zone.

In Fig. 24, the effect of *workpiece rotating speed* on surface roughness (Ra) is shown at *focused and various upward defocusing conditions*. The other process parameters were kept constant at *average power* at 8 W, *pulse frequency* of

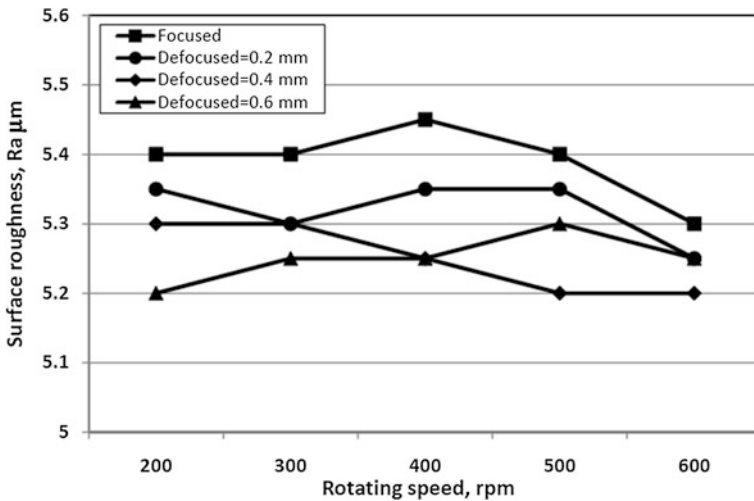


Fig. 24 Variation of surface roughness (Ra) with rotating speed at focused and various upward defocus conditions

5000 Hz and Y feed rate of 0.4 mm/s. From this plot, it is observed that surface roughness values are less for the micro-turned surface machined at *defocused positions* compared to *focused conditions*. It is known that at various *defocused conditions*, the irradiated laser beam energy density is less; therefore, the heights of micro-peaks generated on the machined surface are less. It is also revealed that increase of *rotating speed* results in lower values of surface roughness. It is due to the fact that increase of *rotating speed* results in increase of *circumferential overlap* value according to Eq. 4. Therefore, more even surface is achieved. Moreover, higher *defocused conditions* result in higher surface finish and it is mainly due to melting and instant solidification of workpiece material on the machined surface.

Figure 25 shows the effect of Y feed rate on surface roughness (R_a) at focused and various *upward defocusing conditions*. The other process parameters were kept constant at *average power* of 8 W, *workpiece rotating speed* of 400 rpm and *pulse frequency* of 5000 Hz. It is evident from this plot that the increase of Y feed rate results in deterioration of surface finish of work sample. As increase of Y feed rate results in reduction in *circumferential overlap* over two successive laser scan tracks and this phenomenon creates uneven surface profile over the micro-turned surface and therefore, the roughness of machined surface deteriorated. It is also observed that the surface roughness (R_a) is high at *focused condition* laser micro-turning operation compared to machining at all *defocused positions*. With the increase of defocusing of the laser beam, the laser beam energy density decreases, and as a result, the material removal from the workpiece surface is less.

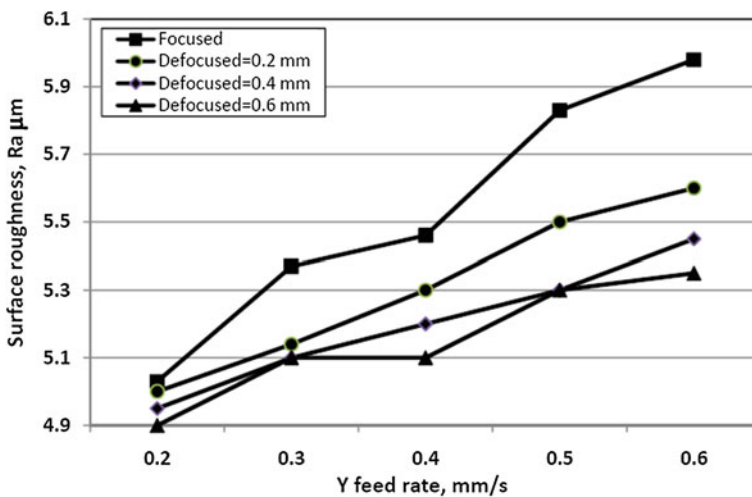


Fig. 25 Variation of surface roughness (R_a) with Y feed rate at focused and various upward defocus conditions

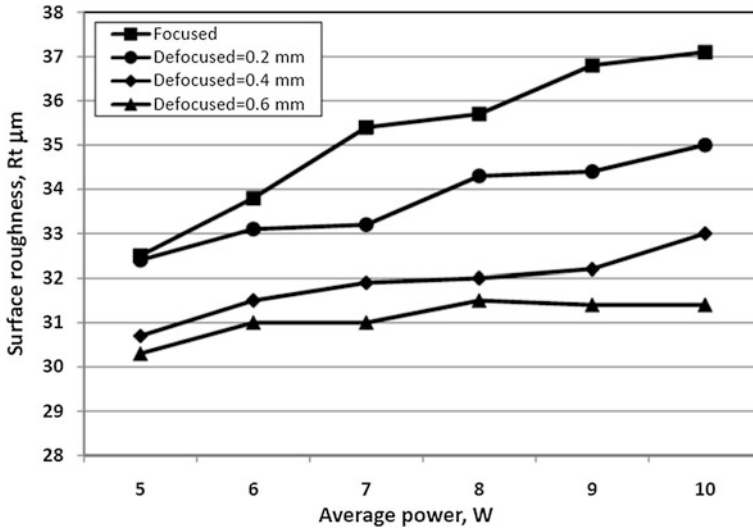


Fig. 26 Variation of surface roughness (Rt) with average power at focused and various upward defocus conditions

In Fig. 26, the effect of *average power* on surface roughness (Rt) is shown at *focused* and various *upward defocusing conditions*. The other process parameters were kept constant as same as Fig. 22. From this plot, it is revealed that with the increase of *average power*, the surface roughness (Rt) is slightly increases and it is due to generation of micro-peaks and valley on the machined surface. It is also observed from the same plot that *defocused condition* machining results in lower value of surface roughness compared to surface roughness (Rt) achieved during machining at *focused condition*. However, at higher value of defocused machining i.e. at 0.4 and 0.8 mm defocusing, the *average power* has no such effect on Rt values.

Figure 27 shows the effect of *pulse frequency* on surface roughness (Rt) at *focused* and various *upward defocusing conditions*. The other process parameters were kept constant as same as Fig. 23. It is evident from this plot that surface roughness (Rt) slightly increases at *focused condition* machining. However, there is no such increment of Rt value of the machined surface at *defocused conditions*. Rt value lie in the range of 30–33 μm . Moreover, the values of Rt is less at *defocusing conditions* compared to machining at *focused position*.

In Fig. 28, the effect of *workpiece rotating speed* on surface roughness (Rt) is shown at *focused* and various *upward defocusing conditions*. The other process parameters were kept constant as same as Fig. 24. It is observed from Fig. 28 that with the increase of *workpiece rotating speed*, surface roughness value decreases.

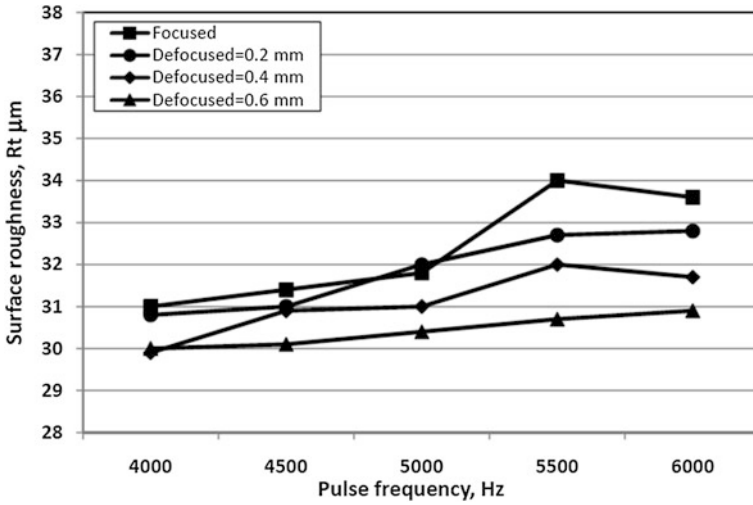


Fig. 27 Variation of surface roughness (Rt) with pulse frequency at focused and various upward defocus conditions

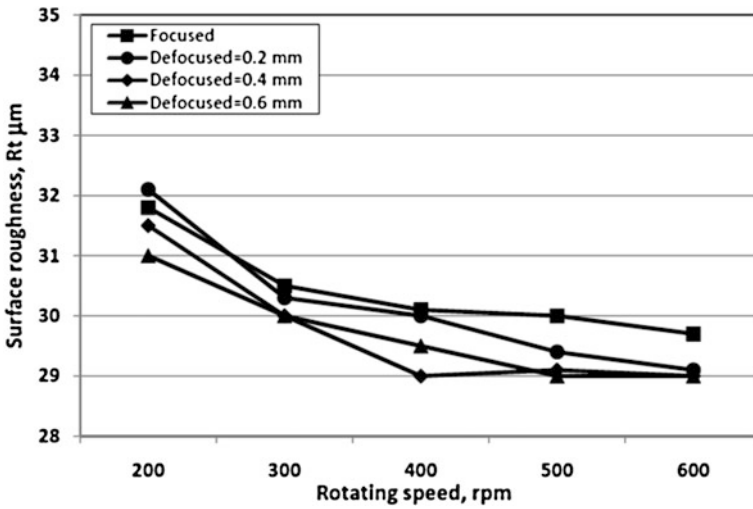


Fig. 28 Variation of surface roughness (Rt) with rotating speed at focused and various upward defocus conditions

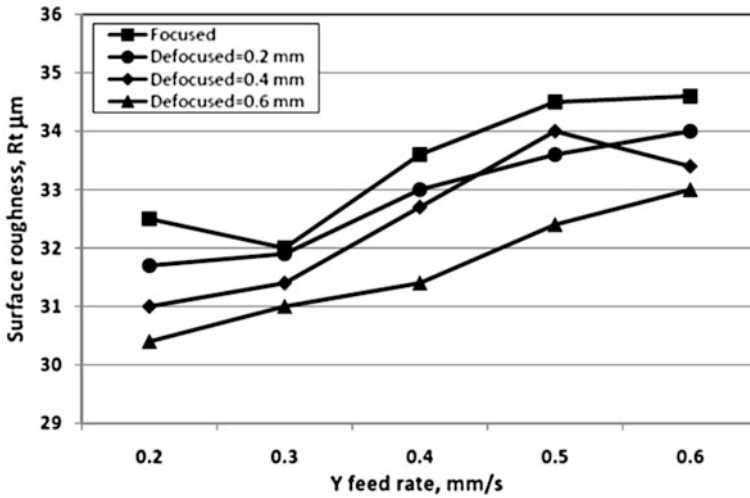


Fig. 29 Variation of surface roughness (Rt) with Y feed rate at focused and various upward defocus conditions

It is mainly due to the increase of *circumferential overlap percentage* during machining. From this plot, it is also revealed that there is no such effect of amount of *defocusing conditions*. However, the value of Rt is higher at *focused condition* compared to machining at *defocused conditions*. Figure 29 shows the effect of *Y feed rate* on surface roughness (Rt) at *focused* and various *upward defocusing conditions*. The other process parameters were kept constant as same as Fig. 25. The figure depicts that the increase of *Y feed rate* results in increase of Rt values at focused as well as all *defocused machining conditions*. It is due to decrease of *circumferential overlap percentage* according to Eq. 4. The values of Rt are less at *defocused machining conditions* compared to *focused machining*.

To analyse the laser micro-turned surface qualitatively, Scanning Electron Microscopic (SEM) images were captured for the surfaces machined at various parametric combinations. In Fig. 30, the exhibited photographs show the surfaces obtained through laser micro-turning on alumina at parametric setting of *average power* of 8 W, *workpiece rotating speed* of 400 rpm and *pulse frequency* of 5000 Hz, *Y feed rate* of 0.4 mm/s both at *focused* and *defocused machining condition*. The surface roughness (Ra) values are 5.46 and 5.1 μm , respectively for *focused* and *defocused (=0.6 mm)* *machining conditions*. The corresponding Rt values are 33.6 and 31.4 μm , respectively. From these figures and obtained results of Ra and Rt, it is obvious that laser micro-turned surface obtained at *defocused machining conditions* are qualitatively high compared to *focused machining condition*. There are lots of micro-peaks observed on the laser micro-turned surface obtained during *focused condition machining*.

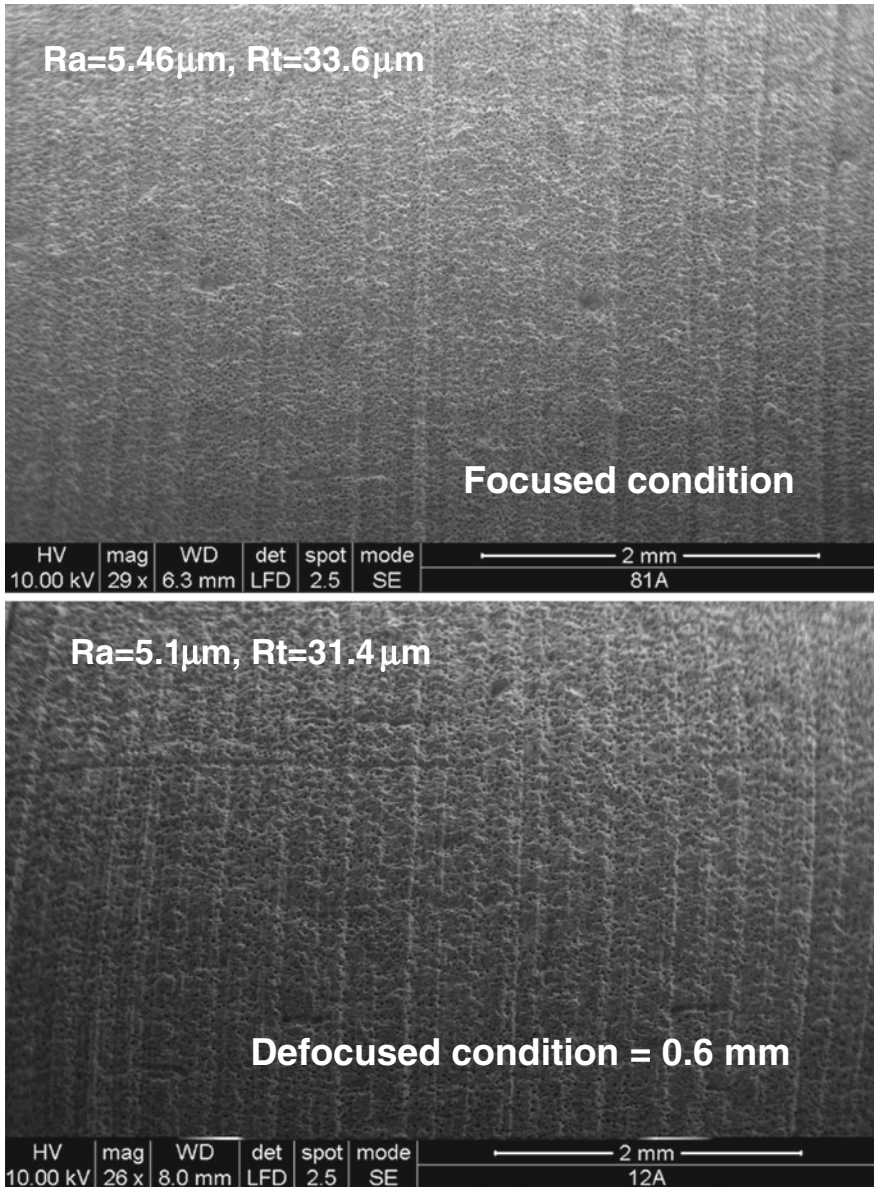


Fig. 30 SEM views of laser micro-turning surfaces machined at average power of 8 W, workpiece rotating speed of 400 rpm and pulse frequency of 5000 Hz, Y feed rate of 0.4 mm/s

7 Conclusions

The pulsed Nd:YAG laser machining system has the competence to perform micro machining process like laser micro-turning operations on difficult-to-machine ceramic materials such as aluminum oxide (Al_2O_3) to achieve a particular depth and surface finish of the cylindrical workpiece. In this chapter, Nd:YAG laser micro-turning operation has been successfully performed to produce laser micro-turning surface up to desired depth on cylindrical workpiece of aluminium oxide (Al_2O_3) ceramic. By proper controlling of the various laser beam parameters like *average power* and *pulse frequency* and various process parameters like *workpiece rotating speed*, *assist air pressure* and *Y feed rate*, the desired machined surface features like accurate dimensional aspect in terms of micro-turning depth and surface roughness were achieved. The present set of research findings will open up new insights and directions to the fundamental and applied research in the area of laser micro-turning to achieve and improve the accuracy, repeatability and finally the reliability of this novel material machining technique in the context of cylindrical micro part fabrication in modern shop floor. The present chapter opens up further future scope of research work related to analysis of surface structure, surface morphology and micro-hardness of the machined surface during laser micro-turning process of various engineering ceramic materials such as zirconia (ZrO_2), aluminium titanate (Al_2TiO_5), magnesia (MgO_2) and silicon nitride (Si_3N_4) under various process parametric conditions. Laser micro-turning can be carried out for examining the phase transformation as well as crack formation on laser micro-tuned surface at various machining conditions.

Acknowledgments The authors acknowledge the financial support and assistance provided by CAS Ph-IV programme of Production Engineering Department of Jadavpur University under University Grants Commission (UGC), New Delhi, India.

References

- Basu, B., & Balani, K. (2010). *Sintering of Ceramics, in Advanced Structural Ceramics*, Wiley-American Ceramic Society (1st ed.). Hoboken: Wiley.
- Buttery, T. C., Statham, A., Percival, J. B., & Hamed, M. S. (1979). Some effects of dressing on grinding performance. *Wear*, 55, 195–219.
- Chrysolouris, G., Bredt, J., Kordas, S., & Wilson, E. (1988). Theoretical aspects of a laser machine tool. *Journal of Engineering for Industry*, 110, 65–70.
- Dahotre, N. B., & Harimkar, S. P. (2008). *Laser Fabrication and Machining of Materials* (1st ed.). Berlin: Springer.
- Dhupal, D., Doloi, B., & Bhattacharyya, B. (2008). Pulsed Nd:YAG laser turning of micro-groove on aluminum oxide ceramic (Al_2O_3). *International Journal of Machine Tools and Manufacture*, 48, 236–248.
- Gadelmawla, E. S., Koura, M. M., Maksoud, T. M. A., Elewa, I. M., & Soliman, H. H. (2002). Roughness parameters. *Journal of Materials Processing Technology*, 123, 133–145.

- Gitzen, W. H. (1970). *Alumina as a Ceramic Material* (1st ed.). USA: Wiley-American Ceramic Society.
- Haddad, M. J., & Tehrani, A. F. (2008). Investigation of cylindrical wire electrical discharge turning (CWEDT) of AISI D3 tool steel based on statistical analysis. *Journal of Materials Processing Technology*, 198, 77–85.
- Haddad, M. J., Alihoseini, F., Hadi, M., Hadad, M., Tehrani, A. F., & Mohammadi, A. (2010). An experimental investigation of cylindrical wire electrical discharge turning process. *International Journal of Advanced Manufacturing Technology*, 46, 1119–1132.
- Kibria, G., Doloi, B., & Bhattacharyya, B. (2010a). Optimization of Nd:YAG laser micro-turning process using response surface methodology. *Proceedings of the 3rd International and 24th All India Manufacturing Technology, Design and Research Conference* (pp. 333–338), December 13–15, 2010, Visakhapatnam.
- Kibria, G., Doloi, B., & Bhattacharyya, B. (2010b). Experimental analysis on Nd:YAG laser micro-turning of alumina ceramic. *International Journal of Advanced Manufacturing Technology*, 50, 643–650.
- Kibria, G., Doloi, B., & Bhattacharyya, B. (2012). Optimisation of Nd:YAG laser micro-turning process using response surface methodology. *International Journal of Precision Technology*, 3, 14–36.
- Kibria, G., Doloi, B., & Bhattacharyya, B. (2013a). Experimental investigation and multi-objective optimization of Nd:YAG laser micro-turning process of alumina ceramic using orthogonal array and grey relational analysis. *Journal of Optics and Laser Technology*, 48, 16–27.
- Kibria, G., Doloi, B., & Bhattacharyya, B. (2013b). Predictive model and process parameters optimization of Nd:YAG laser micro-turning of ceramics. *International Journal of Advanced Manufacturing Technology*, 65, 213–229.
- Kibria, G., Doloi, B., & Bhattacharyya, B. (2014a). Parametric study and optimization of Nd:YAG laser micro-turning process of different grade of alumina ceramics based on Taguchi methodology. *International Journal of Surface Engineering and Interdisciplinary Materials Science*, 2, 15–46.
- Kibria, G., Doloi, B., & Bhattacharyya, B. (2014b). Investigation into the effect of overlap factors and process parameters on surface roughness and machined depth during micro-turning process with Nd:YAG laser. *Journal of Optics and Laser Technology*, 60, 90–98.
- Kibria, G., Doloi, B., & Bhattacharyya, B. (2015). Investigation and analysis on pulsed Nd:YAG laser micro-turning process of aluminium oxide (Al_2O_3) ceramic at various laser defocusing conditions. *International Journal of Advanced Manufacturing Technology*, 76(1–4), 17–27.
- Kim, S. H., Sohn, I. B., & Jeong, S. (2009). Ablation characteristics of aluminum oxide and nitride ceramics during femtosecond laser micromachining. *Applied Surface Science*, 255, 9717–9720.
- Kruth, J. P., Yasa, E., Vanparys, M., & Vaerenbergh J. V. (2007). The enhancement of micro-machining ability of selective laser melting by selective laser erosion. *Proceedings of the International Conference on Polymers and Moulds Innovations*, PMI Gent, Belgium.
- Samant, A. N., & Dahotre, N. B. (2008a). Ab initio physical analysis of single dimensional laser machining of silicon nitride. *Advanced Engineering Materials*, 10, 978–981.
- Samant, A. N., & Dahotre, N. B. (2008b). Computational predictions in single-dimensional laser machining of alumina. *International Journal of Machine Tools and Manufacture*, 48, 1345–1353.
- Shih, A. J. (2000). An experimental investigation of rotary diamond truing and dressing of vitreous bond wheels for ceramic grinding. *International Journal of Machine Tools and Manufacture*, 40, 1755–1774.
- Thawari, G., Sarin Sundar, J. K., Sundararajan, G., & Joshi, S. V. (2005). Influence of process parameters during pulsed Nd:YAG laser cutting of nickel-base superalloys. *Journal of Materials Processing Technology*, 170, 229–239.